Chapter

The Site of Lesion in Hearing Loss: Advances in Otoneuroradiology

Giorgio Conte, Silvia Casale, Sara Sharaini, Federica Di Berardino and Diego Zanetti

Abstract

The last decade has witnessed significant advances in imaging of the middle and inner ear and the auditory pathways. High resolution computerized tomography (CT) scanners and new magnetic resonance (MR) sequences have been implemented in clinical practice as valuable supportive tools for the Audiologist in the identification of the site of lesion and for the surgical planning by the Otologist. The purpose of this chapter is to review the current advanced methods of neuroradiological evaluation of patients with sensorineural hearing loss (SNHL), either congenital or acquired, especially focusing on the assessment of candidates to cochlear implantation (CI), with plenty of explicative images.

Keywords: sensorineural hearing loss, congenital inner ear malformations, acquired inner ear disorders, flat panel CT, high-resolution MR-sequences

1. Introduction

The imaging assessment of the inner ear and the auditory pathway requires high-resolution techniques because their anatomical structures are small and complex. In the last 10 years, computed tomography (CT) and magnetic resonance (MR) has reached much higher spatial resolution for bony and neural structures.

Multi-section CT (MSCT) is the technique of choice for the study of the temporal bone, thanks to its high spatial resolution. However flat panel CT (FPCT) constitutes the newest alternative technique, since it guarantees some additional advantage compared with MSCT in terms of ultra-high isotropic spatial resolution (~150 × 150 × 150 μm^3) and reduction of the effective dose of up to 40% [1–3].

On the other hand, 3 Tesla MR scanners, thanks to the high-resolution sequences such as tridimensional (3D) T2 weighted sequence (3D-T2w, spatial resolution: 0.4 × 0.4 × 0.6 mm^3, field of view: 140 × 140 mm, time of scan: 5′ 32″) and 3D Fluid Attenuated Inversion Recovery (FLAIR), have provided new insight to detect changes in the inner ear [4, 5]. MR is technique of choice to study the peripheral and central auditory pathways.

The purposes of this chapter is to review the state of the art of pre-operative neuroradiological assessments of patients with sensorineural hearing loss (SNHL) especially focusing on candidates to a cochlear implant (CI). Advanced imaging of the morphology and the integrity of anatomical structures will be presented in order to show the current capabilities of correct site of lesion identification.

2. Inner ear and cochlear-vestibular nerve

2.1 Congenital disorders

Inner ear can be affected by malformative and acquired anomalies, which can cause profound to severe hearing impairment. FPCT scan is more accurate than conventional MSCT in the morphologic evaluation of inner ear; FPCT allows an excellent examination of the 32-mm spiral canal of the snail-shaped cochlea, that winds 2 and ½ turns around the modiolus. These turns are separated by interscalar septa, where defects of it and of the modiolus can describe different types of incomplete partition of the cochlea. Sennaroğlu and Bajin summarized the findings of abnormalities involving each inner ear structure, as described in **Table 1** [6].

The most common cochlea anomalies are incomplete partition type I (IP-I) and incomplete partition type II (IP-II). In the IP-I, the cochlea results in a cystic appearance, due to the lack of the entire modiolus and the cribriform area, associated with a large cystic vestibule. In the IP-II (classic Mondini deformity), the cochlea forms a cystic apex, due to the coalescence of the middle and the apical turns, accompanied by a dilated vestibule and enlarged vestibular aqueduct (**Figure 1**). A rare disorder associated with congenital mixed hearing loss is incomplete partition type III, an X-Linked inner ear anomaly, caused by the absence of the bony modiolus and of the septum between the base of the cochlea and the internal auditory canal, with no associated anomalies in the vestibular structures of the inner ear (**Figure 2**) [6, 7]. This anomaly is associated with fixed stapes footplate, which represents a surgical risk of perilymph gusher during stapedectomy, and it represents even a risk of misdirected insertion of the cochlear electrode through the internal acoustic canal, inside the cerebellopontine angle against the brain stem, during cochlear implantation (**Figure 3**).

Cochlear malformations can be accompanied by anomalies of the vestibule or of the semicircular canals, resulting in aplasia, hypoplasia or dilatation [8].

Another cause of SNHL is the presence of enlarged vestibular aqueduct described as larger than 1.5 mm at the midpoint in the axial plane between the common crus and the external aperture, associated with a normal cochlea, vestibule and semicircular canals [8]. The Pöschl projection improves the accuracy in the measurement of the aqueduct. It is defined as 45° from either the sagittal or coronal

Type of IEM	Radiological findings
Complete labyrinthine aplasia	Absent labyrinth
Rudimentary otocyst	Incomplete millimetric otic capsule remnant
Cochlear aplasia	Absent cochlea
Common cavity	Round or ovoid cystic structure for cochlea and vestibule
Cochlear hypoplasia	Cochlear size small
Incomplete partition—I	Cystic cochlea
Incomplete partition—II	Cystic cochlea apex
Incomplete partition—III	Modiolus absent, interscalar septa present
Enlarged vestibular aqueduct	Normal cochlea with enlarged vestibular aqueduct
Cochlear acqueduct abnormalities	Narrow or absent cochlear acqueduct

Table 1.
Sennaroğlu and Bajin's description of the findings of abnormalities involving inner ear structures.

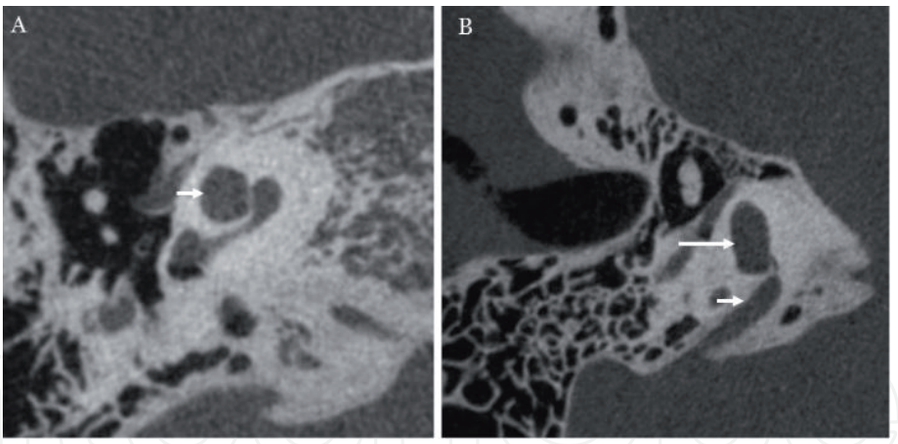

Figure 1.
FPCT on axial plane showing IP-II deformity (classic Mondini deformity): the cochlea forms a cystic apex, due to the fusion of the middle and the apical turns (arrow, A), accompanied by a dilated vestibule (long arrow, B) and enlarged vestibular aqueduct (short arrow, B).

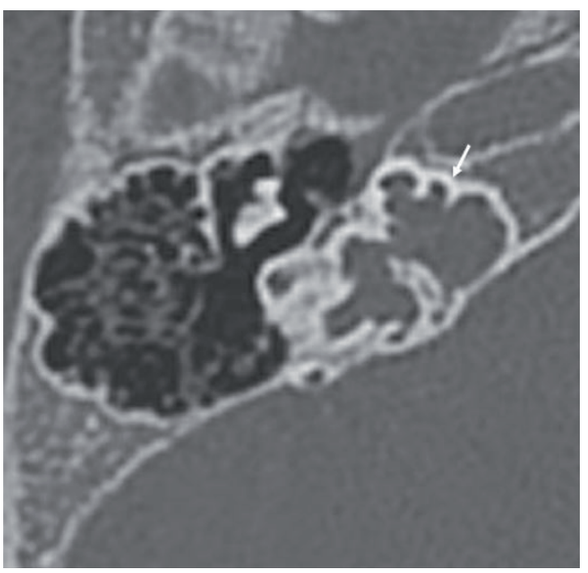

Figure 2.
FPCT on axial plane showing IP-III deformity (arrow), caused by the absence of the bony modiolus and of the septum between the base of the cochlea and the internal auditory canal.

planes or perpendicular to the long axis of the pyramid, or parallel to the superior semicircular canal (**Figure 4**) [9].

Enlarged vestibular aqueduct, accompanied by enlarged endolymphatic sac, can be associated with other cochlear and vestibular anomalies, which can affect therapeutic strategies: scalar asymmetry with enlargement of anterior chamber composed of the scala vestibuli and the scala media, or modiolar deficiency that shows a flattened and attenuated modiolus, well evaluated in 3D-T2w (**Figure 5**).

It is important to identify the atresia or the hypoplasia of the cochlear canal, by measuring the length and the width of the bony canal of the cochlear nerve, respectively obtained by drawing a perpendicular line from the base of the modiolus to the inner margin of the fundus of the internal auditory canal (IAC) and by drawing a line along the inner bony margins (**Figure 6**). The measurements can detect a hypoplastic bony canal, which may be indicative of a embryologic malformation of the cochlear-vestibular nerve (CVN), in patients with congenital SNHL [10–12].

The presence of aplasia or hypoplasia of the CVN must be ruled out since may affect the choice of surgical technique and CI device, as well as the performance

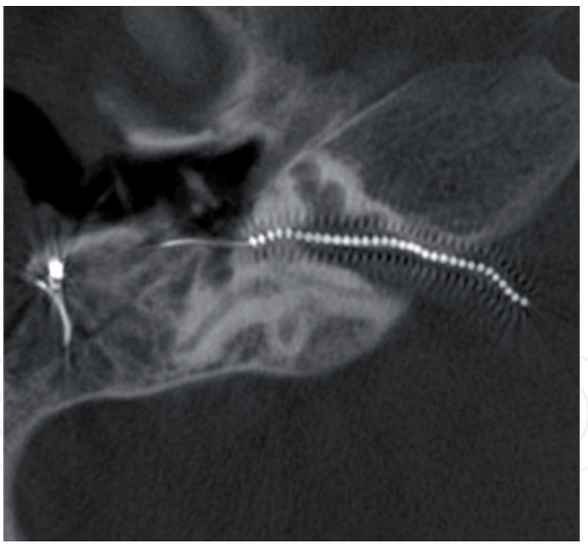

Figure 3.
FPCT on axial plane showing a complicated insertion of cochlear implant in IP-III deformity. The CI electrode enters the internal acoustic canal, reaching the cerebellopontine angle.

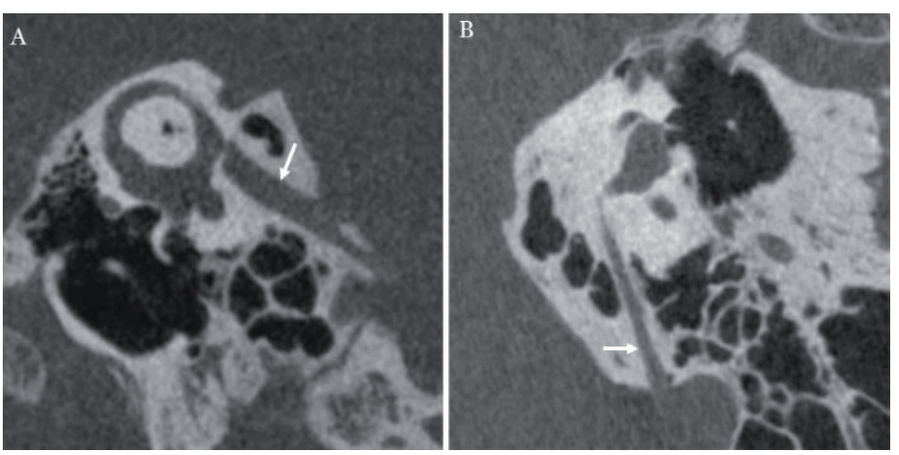

Figure 4.
FPCT on Pöschl projection (A), which is reconstructed approximately 45° from either the sagittal and coronal planes, parallel to the loop of the superior semicircular canal, and axial plane (B) between the common crus and the external opening, showing an enlarged vestibular aqueduct (arrows).

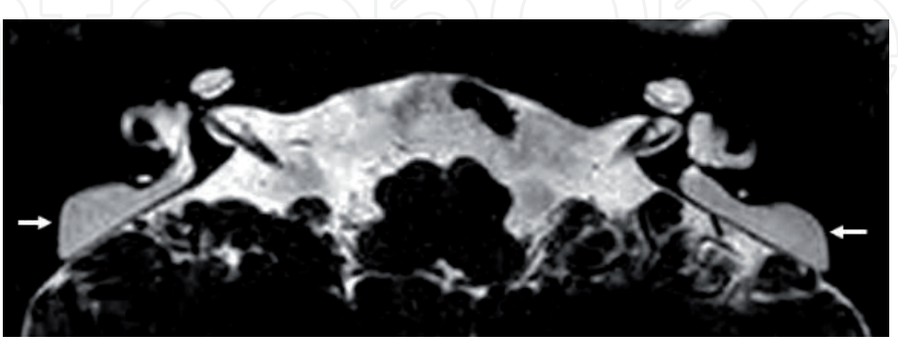

Figure 5.
3D-T2w on 3 Tesla MR on axial plane showing enlarged endolymphatic sacs (arrows), associated with enlarged vestibular aqueducts.

outcome following CI; in patients whose cochlear nerves are missing, an auditory brain stem implant should be considered [13].

The presence of a normal cochlea does not exclude the agenesis of the cochlear nerve because of the different embryogenesis of the otic labyrinth and its neural

elements. Nevertheless the cochlear nerve malformations are often associated with labyrinthine abnormalities [10]. As mentioned above, the hypoplasia of the cochlear canal seen on CT scan is a sensitive indicator of CVN malformation: in that case the CT evaluation should be always followed by MR examination since the 3D-T2w is the most valuable tool to assess nerves anomalies.

The relationship between the facial and the CVN within the IAC may vary among individuals (**Figures 7** and **8**).

2.2 Acquired disorders

Among acquired lesions in SNHL, the presence and the extension of a labyrinthine ossification represents another great challenge for the surgeon, owing to difficult insertion of the electrode array. It may occur like "end-stage" of different labyrinthine pathologies, categorized as infective or non-infective, including meningitis, otitis media, trauma, otosclerosis and labyrinthectomy. Fibrosis can precede ossification but extensive fibrosis without ossification rarely occurs. The

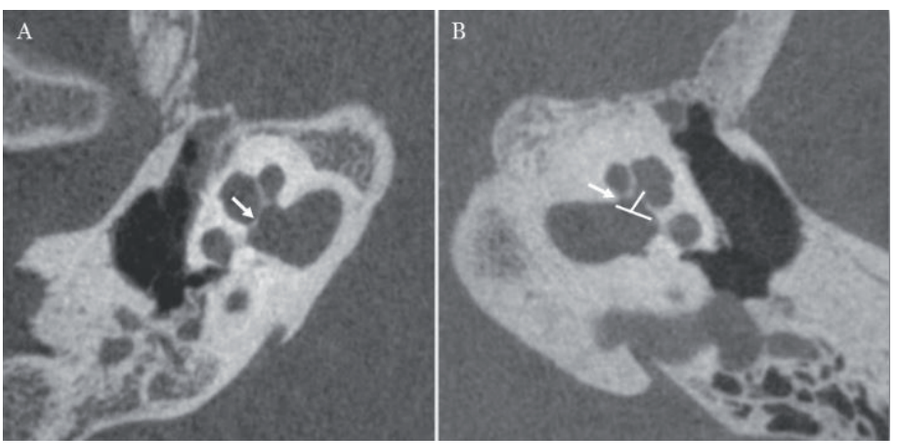

Figure 6.
FPCT on axial plane showing aplasia of cochlear canal (arrow, A) and normal cochlear canal (arrow, B). The measurement of the length and the width of the bony cochlear canal are made by drawing a perpendicular line from the base of the modiolus to the inner margin of the fundus of the internal acoustic meatus and by drawing a line along the inner margins of its bone edges (B).

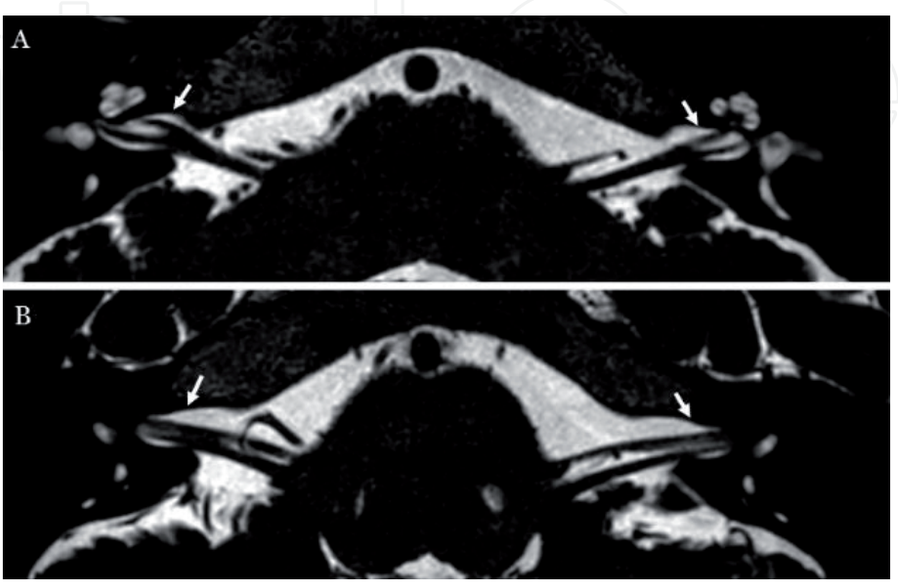

Figure 7.
3D-T2w on 3 Tesla MR on axial plane showing normal appearance of cochlear and inferior vestibular nerves (arrows, A), facial and superior vestibular nerves (arrow, B).

stage of fibrosis begins ~2 weeks after the onset of infection, but CT images remains elusive. Instead, 3D-T2w demonstrates replacement of the normally fluid-filled spaces of the labyrinth, resulting in reduced T2w signal and shows the presence of labyrinthine enhancement after gadolinium. MR images have the advantage of not only diagnosing cochlear obstruction, but even better sensitivity for estimating the extent of fibrous obstruction, subtle at CT images, thus allowing earlier diagnosis (**Figures 9** and **10**) [14].

The end stage of the ossification results in the absence of T2w signal of the labyrinth; this stage is also well seen from CT images (**Figure 11**).

Reduced T2w signal is reported in vestibular schwannoma, up to 10–20% of the causes of SNHL, but it always results in intralabyrinthine contrast enhancement (**Figure 12**).

The management of far advanced otosclerosis may represent another important objective in the era of CI [15]. In the original otosclerosis, the aberrant bone deposition around the stapes footplate results in the impairment of the mechanical transmission of sound, leading to conductive hearing loss. In advanced otosclerosis,

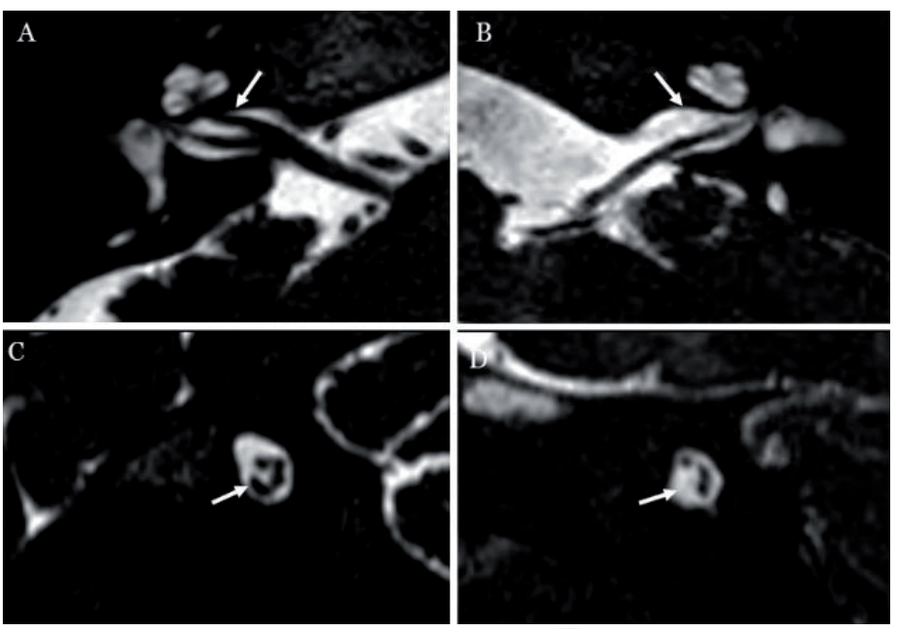

Figure 8.
3D-T2w on 3 Tesla MR showing normal appearance of cochlear nerve on axial (arrow, A) and sagittal plane (arrow, C) and aplasia of cochlear nerve on axial plane (arrow, B) and on sagittal plane (arrow, D).

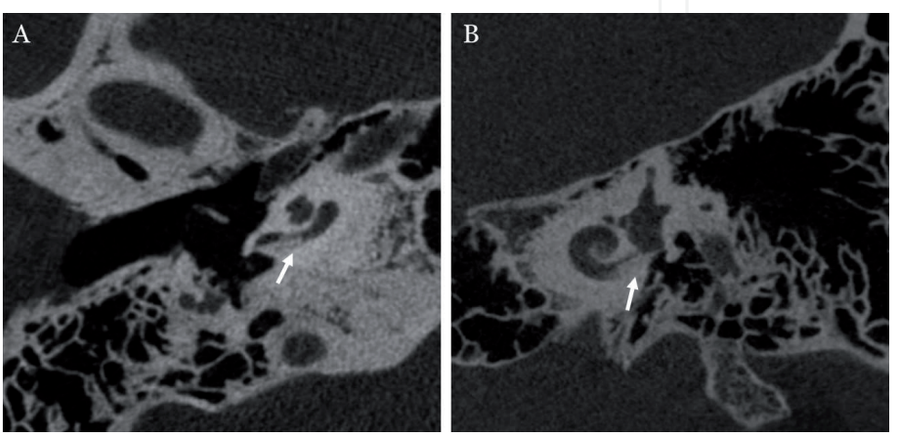

Figure 9.
FPCT on axial (A) and para-coronal (B) planes showing minimal ossification of the basal turn of the cochlea.

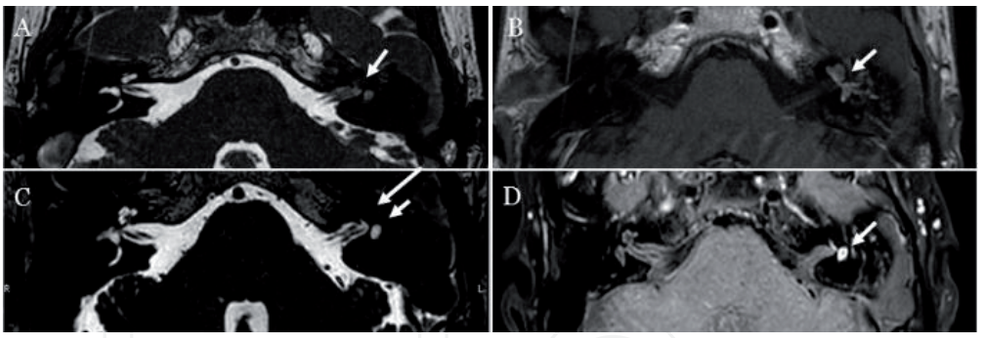

Figure 10.
3-Tesla MR shows loss of signal of the left cochlea and vestibule on axial T2w sequence (arrow, A), and enhancement after contrast-medium administration on axial T1w (arrow, B), suggesting intralabyrinthine fibrosis. At 1-year follow-up, MRI shows loss of signal of the left cochlea on T2w sequence (long arrow, C), without enhancement after contrast-medium administration, compatible with complete ossification; MR findings suggest that active fibrosis is still present within the left vestibule (short arrow, C and D).

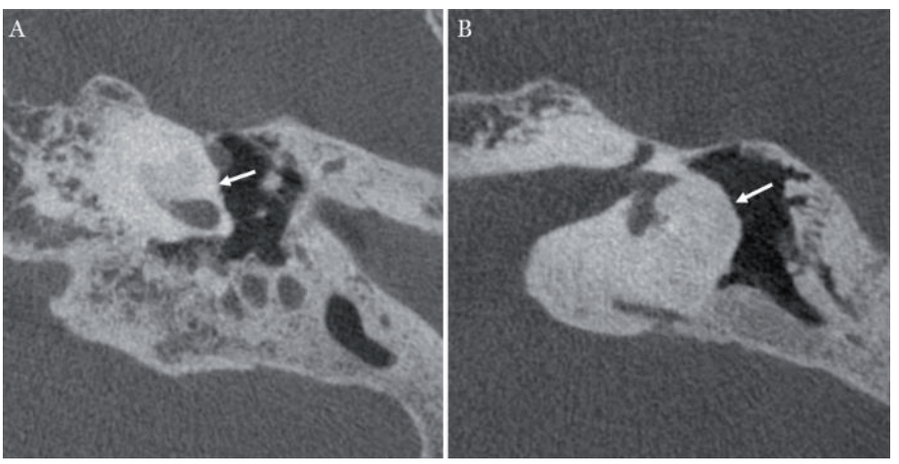

Figure 11.
FPCT on axial plane showing the "end stage" of the ossification of the cochlea (arrow, A) and semicircular lateral canal (arrow, B).

bone deposits can extend into the bony labyrinth of the inner ear, surrounding the cochlea and resulting in a mixed conductive and SNHL. Advanced otosclerosis with cochlear involvement may influence the insertion and the performance of a CI. Despite in these patients the CI has proven to be the most effective treatment modality, endoluminal otospongiotic obstruction may complicate the insertion of the array and alter the spread of the electrical stimulation. Pre-operative CT may clearly detect ossification of the cochlea (**Figure 13**) [16].

Until recently, MR imaging with and without contrast media has been used only to exclude cochlear causes of sudden SNHL (SSHL), such as a vestibular schwannoma, and rare causes of retrocochlear SSHL including demyelinating disease, brain stem infarctions and cerebellopontine tumors.

Nowadays, pre-contrast T1-weighted and 3D-FLAIR sequence may suggest the pathogenesis of SSHL.

Two specific patterns can be identified: the "*vascular*" pattern, characterized by the presence of methemoglobin in the inner ear that appears as hyperintense on both pre-contrast T1-weighted and 3D-FLAIR images (**Figure 14**), and the "*inflammatory*" pattern which shows high signal only on 3D-FLAIR sequence, due to the presence of proteins in the inner ear fluids (**Figure 15**). Both patterns can be associated with enhancement on post-contrast 3D-FLAIR which suggests the blood-labyrinth breakdown [17].

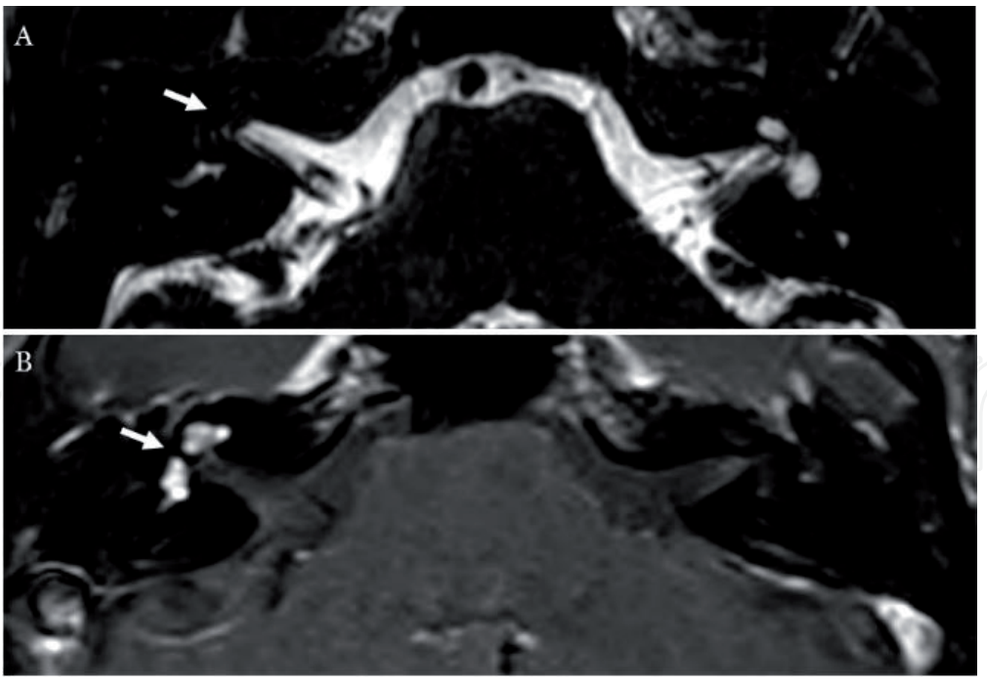

Figure 12.
MR images 3D-T2 (A) showing reduced T2 signal of the right cochlea and vestibule (arrow); after intravenous contrast-medium administration T1w sequence (B) shows cochlear and vestibular enhancement (arrow), due to intralabyrinthine schwannoma.

Figure 13.
FPCT on axial plane shows a peri-cochlear hypodensity (arrow) compatible with advanced otosclerosis.

MR sequences, in particular 3D-T2, are excellent to analyze inner ear fluids intensity, and to investigate the morphology of the inner ear structures, cranial nerve VIII, internal auditory canal and cerebellopontine angle [18, 19].

Post-contrast 3D-FLAIR sequences are able to identify pathological conditions characterized by blood-labyrinth barrier breakdown, including viral infection, immune-mediated inner ear disease, perilymphatic fistulas [20, 21].

Furthermore, the 4 h-delayed 3D-FLAIR sequences on 3 Tesla scanner after intravenous administration of gadolinium-based contrast agent offer enough spatial resolution to detect small endolymphatic structures, such as saccule and utricle; in this sequences the endolabyrinth appears to have a lower signal compared with the surrounding perilymph.

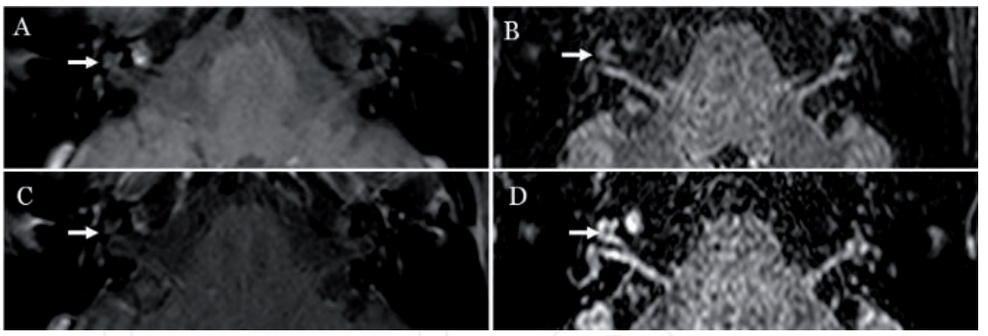

Figure 14.
Vascular pattern of SSHL. Pre-contrast T1w (A) and 3D-FLAIR (B) sequences show a high signal in the right cochlea (arrow), without enhancement on postcontrast T1w (arrow, C). The inner ear enhancement on 3D-FLAIR sequence is consistent with blood-labyrinth barrier breakdown of the inner ear (arrow, D).

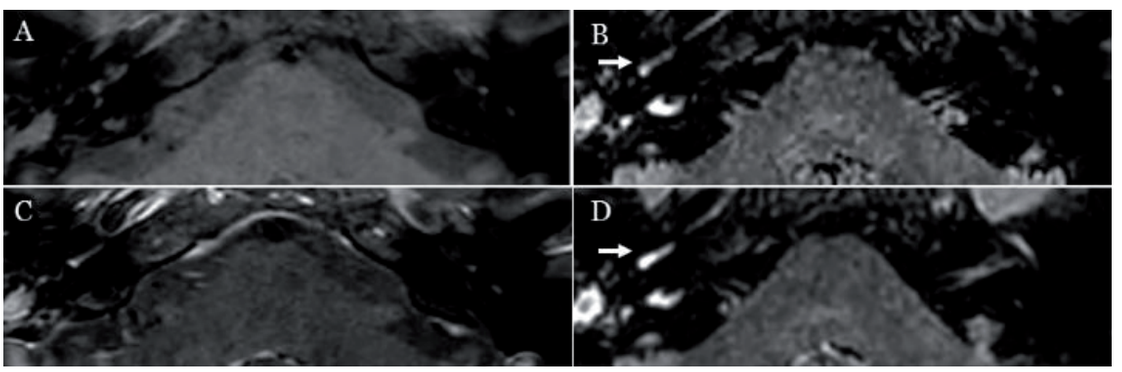

Figure 15.
Inflammatory pattern of SSHL. The pre-contrast T1w (arrow, A) shows no signal abnormalities. The pre-contrast 3D-FLAIR (arrow, B) shows a high signal in the basal turn of the right cochlea. A postcontrast T1-w sequence (arrow, C) does not show enhancement, whereas a postcontrast 3D-FLAIR sequence (arrow, D) shows the basal turn of the cochlea markedly enhanced on the right side.

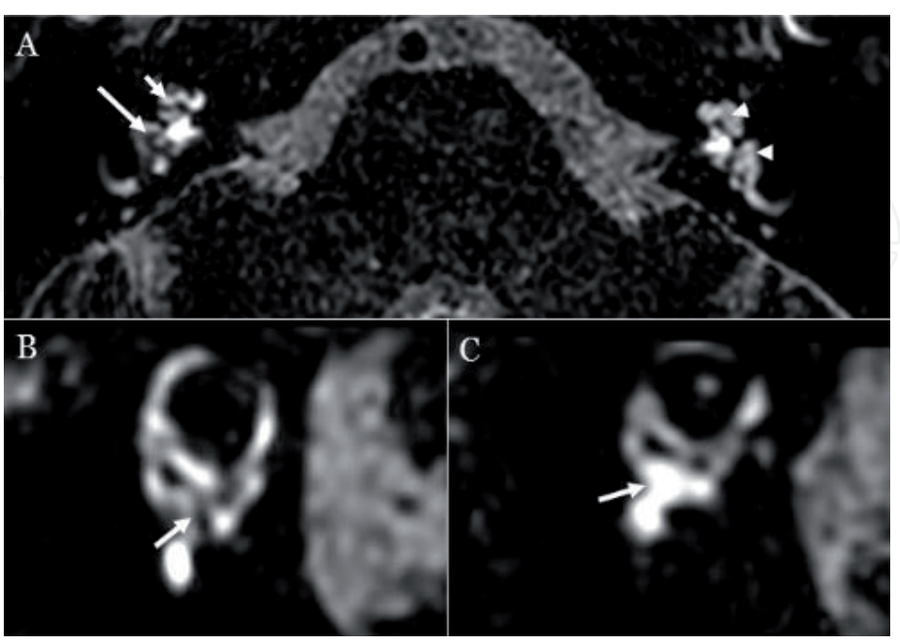

Figure 16.
Axial 3D-FLAIR sequence after 4-h from intravenous contrast-medium administration (A) shows right vestibular (long arrow) and cochlear (short arrow) hydrops, compared with the normal left inner ear (arrowheads). On oblique sagittal plane (B), the 4-h delayed postcontrast 3D-FLAIR sequence confirms the right vestibular endolymphatic hydrops, in particular of the saccule (arrow), while in the left ear (C), the inferior third of the vestibule is normally filled by perilymph (arrow).

In patients with Meniere's disease, the pathological finding is represented by endolymphatic hydrops, characterized by a distension of the endolymphatic space of the inner ear into areas that are normally filled with perilymphatic liquid (**Figure 16**). CI is an effective means of treatment of patients with end-stage Meniere's disease affected by severe-to-profound SNHL [22–24].

3. Auditory central nervous system

The auditory central system includes: the cochlear nucleus and the superior olivary complex in the pons, the inferior colliculus in the midbrain, the medial geniculate nucleus of the thalamus and the auditory cortex (i.e. Heschl's gyrus) in the temporal lobe.

Nowadays, MR imaging is the modality of choice to investigate the auditory central pathway, because of its better sensitivity and specificity compared with others neuro-imaging modalities (CT and, in the newborn, ultrasound scanning).

The auditory pathway myelination begins during the fetal life and increases up to the first year of age, reflecting the improvement of the auditory system function. The changes in myelin can be seen using MR imaging by the 37th fetal week in the brainstem and later in the structure higher in the auditory pathway, as early as 10 weeks of age in the medial geniculate nucleus and by 24 weeks in subcortical white matter (**Figure 17**) [25, 26].

The 3T MR scanner, thanks to its high contrast and spatial resolution, guarantees great sensitivity in the detection of white matter injury, playing an important role in the early diagnosis of some pathologies related with congenital SNHL [27].

In addition to conventional MR sequences, some advanced techniques such as diffusion tensor imaging (DTI) and functional MR imaging (fMRI), may be helpful to provide new insight into structural and functional white matter changes in early stage of congenital SNHL [28]. On the other hand, the investigation of the first step of the central auditory pathway, i.e. cochlear nucleus, is challenging and currently limited in clinical practice. The most promising MR sequences are T2-weighted

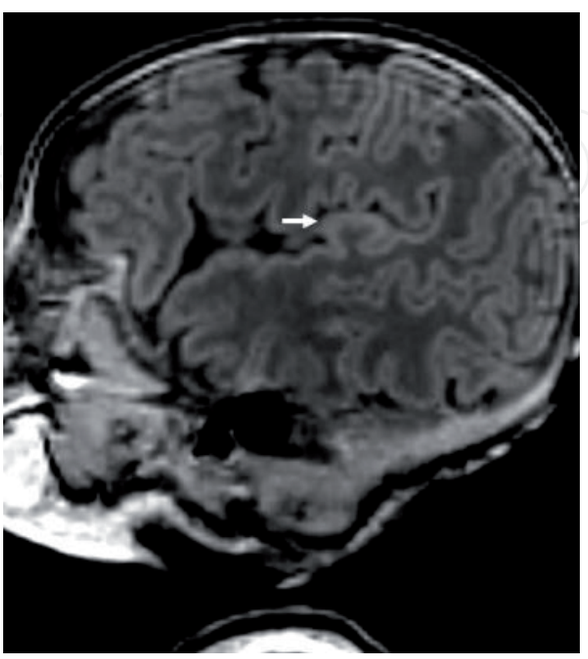

Figure 17.
Sagittal T1w sequence in a healthy 42-weeks newborn shows the normal myelination pattern (as hyper-intense signal) in the cortical rim of the Heschl's girus (arrow).

gradient-echo (T2GE) imaging and susceptibility weighted imaging (SWI), which ensure a good contrast resolution between hypointensity of the nuclei, due to paramagnetic deposition, and hyperintensity of the surrounding myelinated tissue.

Both environmental and genetic pathologies may lead to congenital SNHL, with possible involvement of any component of acoustic pathway [29, 30].

Frequently, the anatomical structure primarily involved in inherited hearing loss are the inner ear and the CNV (discussed in the previous chapter), while the auditory central pathway is spared by any lesion at the conventional MR investigation.

Conversely, the central system is commonly involved in acquired SNHL disorders. Cytomegalovirus (CMV) is the most common congenital non-genetic cause of SNHL [31]. About 10% of CMV infection results in several brain abnormalities. At present, an official guideline on the preferred neuroimaging modalities to identify brain abnormalities in patients with CMV infection is lacking; the current practice varies according to center-based protocols [32].

MR imaging is more sensitive than ultrasound scanning in the detection of mild and severe brain abnormalities, such as: microcephaly, cerebellar hypoplasia, cortical anomalies, calcification, white matter changes, polar temporal lesion,

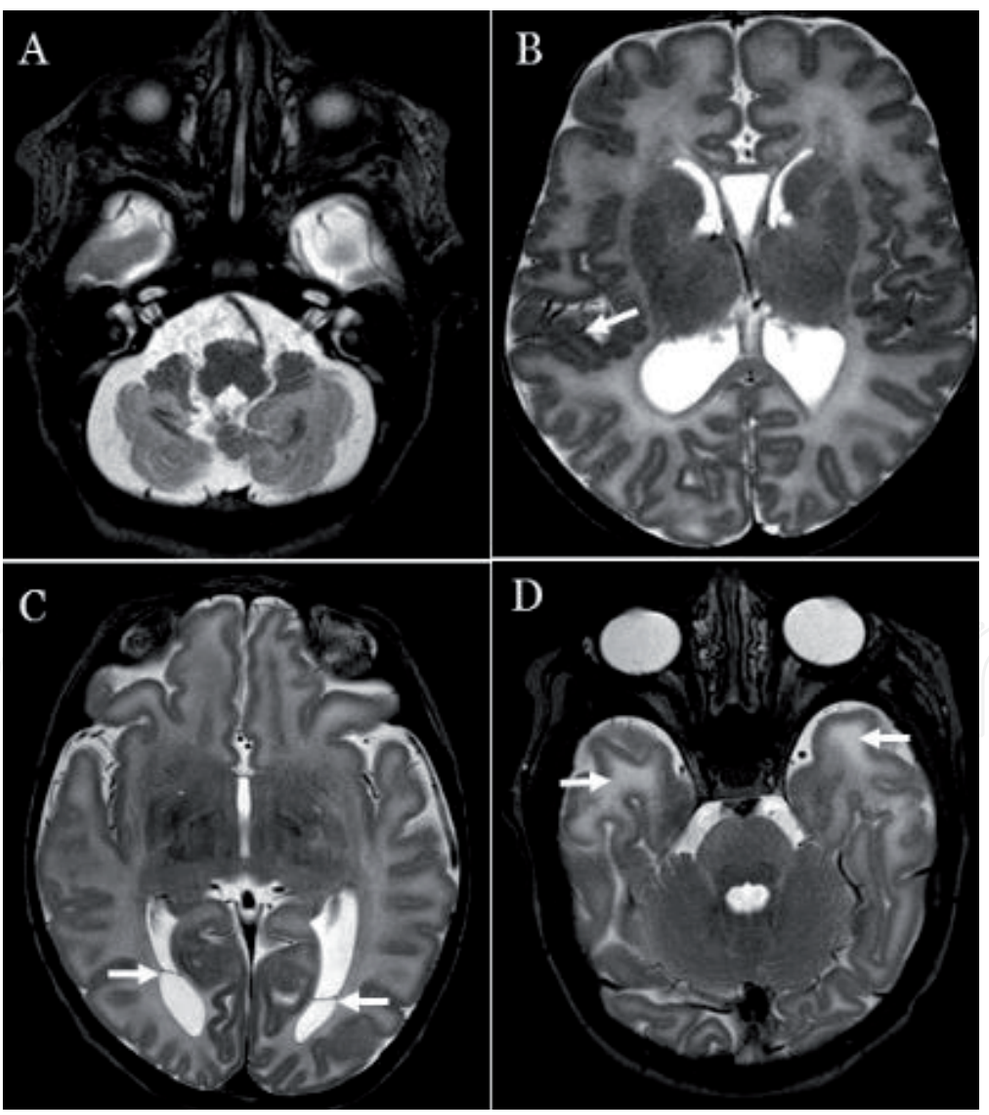

Figure 18.
MR findings in four patients with congenital cytomegalovirus infection: cerebellar hypoplasia (A); perisylvian polymicrogyria (B) that involves the right Heschl's gyrus (arrow); intraventricular septation (C) in the occipital horn of the lateral ventricles (arrows, C); hyperintensity of the anterior temporal white matter (D, arrows).

sub-ependimal cyst, ventriculomegaly and intraventricular septa (**Figure 18**). The combination of these malformations depends on gestation age at time of infection [33, 34].

Unfortunately, up to date no specific MR finding is significantly associated with the hearing impairment and outcome of treatment [35]. Moreover, all the above mentioned findings are common to several conditions associated with SNHL and should be considered in the differential diagnosis.

Considering others congenital infections, toxoplasmosis and rubella are commonly described as sharing similar pictures with CMV. In countries where the rubella immunization programs are in place, a congenital infection is currently rare; nevertheless, this diagnostic hypothesis should be considered in presence of brain calcifications, white matter lesions, intraventricular septations, subependymal germinolytic cysts and ventriculomegaly. Noteworthy, newborns affected by CMV showing with brain abnormalities are usually asymptomatic from a neurological standpoint, but may develop progressive SNHL only later on in life [36, 37].

Other rare causes of acquired hearing loss, occurring whenever the auditory central pathway is involved in the injury, are focal brain lesions following perinatal ischemic or hemorrhagic event may (**Figure 19**), hypoxic-ischemic encephalopathy (HIE) (**Figure 20**) [38, 39]. Therapeutic hypothermia, which is the only approved treatment for HIE, because it reduces the extension of brain lesions, has been unfortunately associated with SNHL. The correlation between imaging and functional outcome is still unknown; up to 10% of the treated babies develop hearing impairment.

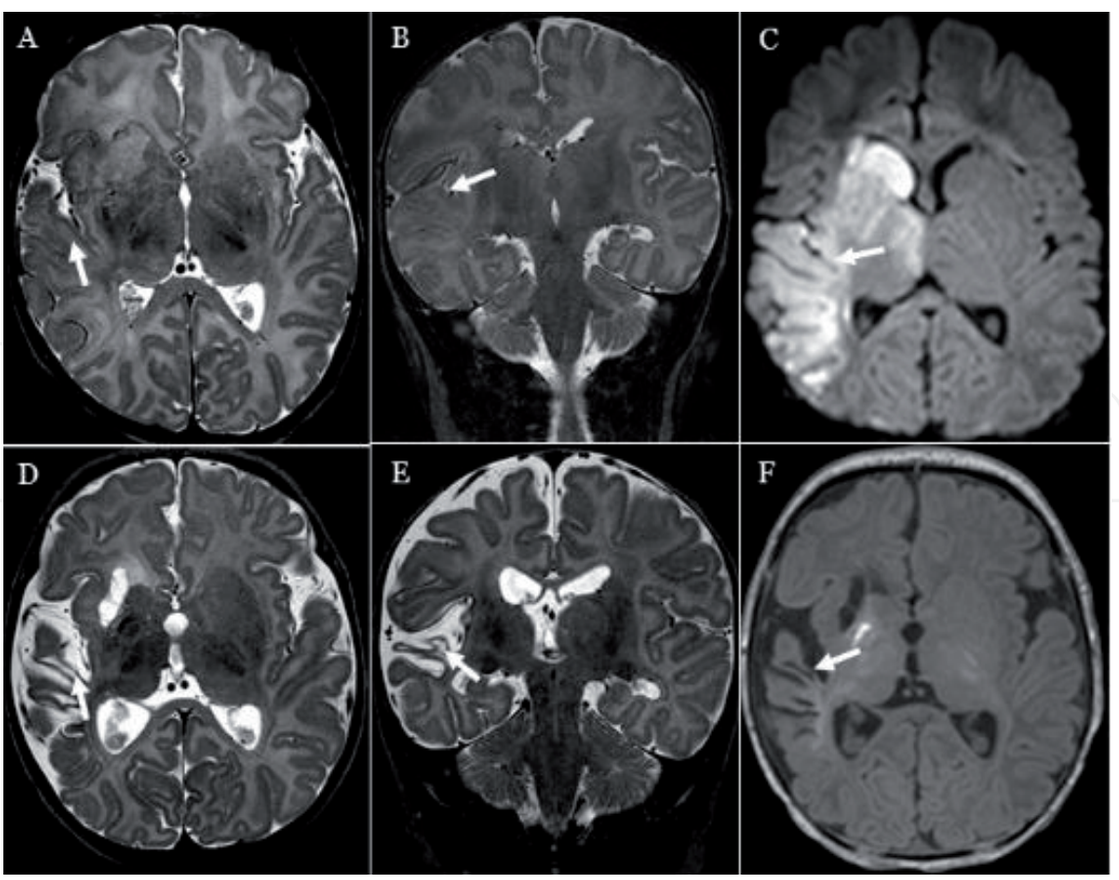

Figure 19.
Images showing the evolution of perinatal ischemic injury involving the right temporal lobe and the right basal ganglia. Axial T2w (A), coronal T2w (B) and DWI (C) images of 2 days newborn during the acute phase of the ischemic injury. Axial T2w (D), coronal T2w (E) and axial T1w (F) images showing the massive damage after 42 days; the involvement of the primary auditory cortex (arrows) caused SNHL.

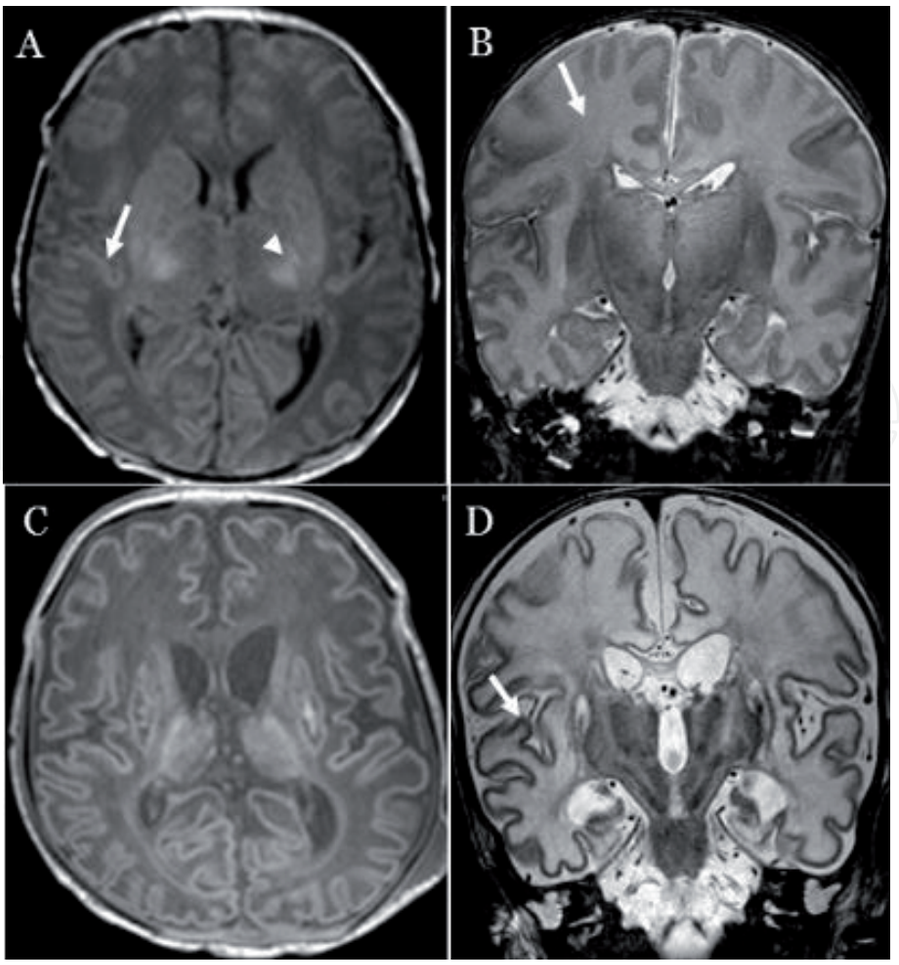

Figure 20.
Images showing the evolution of HIE in a term newborn. In the acute phase, axial T1w section (A) shows hyperintensity of the right Heschl's gyrus (arrow) and mild hyperintensity of the basal ganglia (arrowheads), while the coronal T2w section (B) demonstrates a widely hyperintense white matter (arrow). After 1 week: the axial T1w (C) and coronal T2w (D) sections show chronic changes, with more prominent signal changes in the white matter and basal ganglia and loss of brain matter.

MR studies with DWI sequence are widely used as an early outcome measure after hypothermia.

MR spectroscopy, measuring cerebral metabolites changes, has recently been investigated as a possible tool in predicting neurodevelopmental outcomes in newborn with HIE [40]. In the near future, advanced MR technique might be also used to investigate possible correlation between hypothermia and deafness [41].

In conclusion, the latest neuroimaging techniques play a relevant role in the diagnosis of congenital and acquired disorders underlying SNHL. While advanced MR sequences allow to clarify possible differential diagnoses and to achieve a correct identification of the site of lesion from the inner ear to the auditory cortex, the combination of FPCT and MR undoubtedly support the clinicians in the counseling and management of patient's candidate to CI.

Author details

Giorgio Conte[1], Silvia Casale[2], Sara Sbaraini[3], Federica Di Berardino[4] and Diego Zanetti[4*]

1 Department of Neuroradiology, Fondazione IRCCS Ca' Granda Ospedale Maggiore Policlinico di Milano, Italy

2 Università degli Studi di Pavia, Italy

3 Università degli Studi di Milano, Italy

4 Department of Audiology, Fondazione IRCCS Ca' Granda Ospedale Maggiore Policlinico di Milano, Università degli Studi di Milano, Italy

*Address all correspondence to: diego.zanetti@policlinico.mi.it

IntechOpen

References

[1] Conte G, Scola E, Calloni S, Di Berardino F, Zanetti D, et al. Flat panel angiography in the cross-sectional imaging of the temporal bone: Assessment of image quality and radiation dose compared with a 64-section multisection CT scanner. AJNR. American Journal of Neuroradiology. 2017;**38**(10):1998-2002

[2] Fatterpekar GM, Doshi AH, Dugar M, Delman BN, Naidich TP, Som PM. Role of 3D CT in the evaluation of the temporal bone. Radiographics. 2006;**26**(Suppl 1): S117-S132

[3] Piergallini L, Scola E, Tuscano B, et al. Flat-panel CT versus 128-slice CT in temporal bone imaging: Assessment of image quality and radiation dose. European Journal of Radiology. 2018;**106**:106-113

[4] Conte G, Caschera L, Tuscano B, Di Berardino F, Zanetti D, et al. Three-Tesla magnetic resonance imaging of the vestibular endolymphatic space: A systematic qualitative description in healthy ears. European Journal of Radiology. 2018;**109**:77-82

[5] Fitzgerald DC, Mark AS. Sudden hearing loss: Frequency of abnormal findings on contrast-enhanced MR studies. AJNR. American Journal of Neuroradiology. 1998;**19**(8):1433-1436

[6] Sennaroğlu L, Bajin MD. Classification and current management of inner ear malformations. Balkan Medical Journal. 2017;**34**(5):397-411

[7] Casselman JW, Offeciers EF, De Foer B, Govaerts P, Kuhweide R, Somers T. CT and MR imaging of congential abnormalities of the inner ear and internal auditory canal. European Journal of Radiology. 2001;**40**(2):94-104. DOI: 10.1016/s0720-048x(01)00377-1

[8] Davidson HC, Harnsberger HR, Lemmerling MM, et al. MR evaluation of vestibulocochlear anomalies associated with large endolymphatic duct and sac. AJNR. American Journal of Neuroradiology. 1999;**20**(8):1435-1441

[9] Hwang M, Marovich R, Shin SS, Chi D, Branstetter BF 4th. Optimizing CT for the evaluation of vestibular aqueduct enlargement: Inter-rater reproducibility and predictive value of reformatted CT measurements. Journal of Otology. 2015;**10**(1):13-17

[10] Casselman JW, Offeciers FE, Govaerts PJ, et al. Aplasia and hypoplasia of the vestibulocochlear nerve: Diagnosis with MR imaging. Radiology. 1997;**202**(3):773-781. DOI: 10.1148/radiology.202.3.9051033

[11] Fatterpekar GM, Mukherji SK, Alley J, Lin Y, Castillo M. Hypoplasia of the bony canal for the cochlear nerve in patients with congenital sensorineural hearing loss: Initial observations. Radiology. 2000;**215**(1):243-246

[12] Choi YJ, Sang YP, Myung SK, Ki JS. The significance of a hypoplastic bony canal for the cochlear nerve in patients with sensorineural hearing loss: CT and MRI findings. Journal of the Korean Radiological Society. 2004;**50**(4):227-236

[13] Brackmann DE, Hitselberger WE, Nelson RA, et al. Auditory brainstem implant: I. Issues in surgical implantation. Otolaryngology and Head and Neck Surgery. 1993;**108**(6):624-633

[14] Booth TN, Roland P, Kutz JW, Lee K, Isaacson B. High-resolution 3-D T2-weighted imaging in the diagnosis of labyrinthitis ossificans: Emphasis on subtle cochlear involvement. Pediatric

Radiology. 2013;**50**:1584-1590. DOI: 10.1007/s00247-013-2747-5

[15] Ruckenstein MJ, Rafter KO, Montes M, Bigelow DC. Management of far advanced otosclerosis in the era of cochlear implantation. Otology & Neurotology. 2001;**22**(4):471-474

[16] Calvino M, Sánchez-Cuadrado I, Gavilán J, Lassaletta L. Cochlear implant users with otosclerosis: Are hearing and quality of life outcomes worse than in cochlear implant users without otosclerosis? Audiology and Neurotology. 2018;**23**(6):345-355. DOI: 10.1159/000496191

[17] Conte G, Di Berardino F, Sina C, Zanetti D, et al. MR imaging in sudden sensorineural hearing loss. Time to talk. AJNR. American Journal of Neuroradiology. 2017;**38**(8):1475-1479

[18] Conte G, Di Berardino F, Avignone S, Sina C, Iofrida E, Zanetti D, et al. The "full-blown" MRI of sudden hearing loss: 3D-FLAIR in a patient with bilateral metastases in the internal auditory canals. Neuroradiology Journal. 2018;**31**(1):39-41

[19] Kim HS, Kim DI, Chung IH, Lee WS, Kim KY. Topographical relationship of the facial and vestibulocochlear nerves in the subarachnoid space and internal auditory canal. AJNR. American Journal of Neuroradiology. 1998;**19**(6):1155-1161

[20] Mark AS, Fitzgerald D. Segmental enhancement of the cochlea on contrast-enhanced MR: Correlation with the frequency of hearing loss and possible sign of perilymphatic fistula and autoimmune labyrinthitis. AJNR. American Journal of Neuroradiology. 1993;**14**(4):991-996

[21] Lemmerling MM, De Foer B, Verbist BM, VandeVyver V. Imaging of inflammatory and infectious diseases in the temporal bone. Neuroimaging Clinics of North America. 2009;**19**(3):321-337

[22] Conte G, Lo Russo FM, Calloni SF, Sina C, Barozzi S, Di Berardino F, et al. MR imaging of hydrops in Ménière's disease: All that glitters is not gold. Acta Otorhinolaryngologica Italica. 2018;**38**(4):369-376

[23] Conte G, Caschera L, Calloni S, Di Berardino F, Zanetti D, et al. MR imaging in Menière disease: Is the contact between the vestibular endolymphatic space and the oval window a reliable biomarker? American Journal of Neuroradiology. 2018;**39**(11)59:2114-2119. DOI: 10.3174/ajnr.a5841

[24] Prenzler NK, Bültmann E, Giourgas A, et al. Cochlear implantation in patients with definite Meniere's disease. European Archives of Oto-Rhino-Laryngology. 2017;**274**(2):751-756. DOI: 10.1007/s00405-016-4356-z

[25] Guleria S, Kelly TG. Myelin, myelination, and corresponding magnetic resonance imaging changes. Radiologic Clinics of North America. 2014;**52**(2):227-239

[26] Moore JK, Perazzo LM, Braun A. Time course of axonal myelination in the human brainstem auditory pathway. Hearing Research. 1995;**87**(1-2):21-31

[27] Long P, Wan G, Roberts MT, Corfas G. Myelin development, plasticity, and pathology in the auditory system. Developmental Neurobiology. 2018;**78**(2):80-92

[28] Wang S, Fan G. Alterations of structural and functional connectivity in profound sensorineural hearing loss infants within an early sensitive period: A combined DTI and fMRI study. Developmental Cognitive Neuroscience. 2019;**38**:100654

[29] Korver AMH, Smith RJH, Van Camp G, et al. Congenital hearing

loss. Nature Reviews. Disease Primers. 2017;**3**:16094

[30] Smith RJH, Bale JF, White KR. Sensorineural hearing loss in children. The Lancet. 2005;**365**(9462):879-890. DOI: 10.1016/s0140-6736(05)71047-3

[31] Manicklal S, Emery VC, Lazzarotto T, Boppana SB, Gupta RK. The "silent" global burden of congenital cytomegalovirus. Clinical Microbiology Reviews. 2013;**26**(1):86-102

[32] Smiljkovic M, Renaud C, Tapiero B, Lamarre V, Kakkar F. Head ultrasound, CT or MRI? The choice of neuroimaging in the assessment of infants with congenital cytomegalovirus infection. BMC Pediatrics. 2019;**19**(1):180

[33] Bonifacio SL, Glass HC, Vanderpluym J, et al. Perinatal events and early magnetic resonance imaging in therapeutic hypothermia. The Journal of Pediatrics. 2011;**158**(3):360-365

[34] Doneda C, Parazzini C, Righini A, et al. Early cerebral lesions in cytomegalovirus infection: Prenatal MR imaging. Radiology. 2010;**255**(2):613-621

[35] Kwak M, Yum M-S, Yeh H-R, Kim H-J, Ko T-S. Brain magnetic resonance imaging findings of congenital cytomegalovirus infection as a prognostic factor for neurological outcome. Pediatric Neurology. 2018;**83**:14-18. DOI: 10.1016/j.pediatrneurol.2018.03.008

[36] Severino M, Zerem A, Biancheri R, Cristina E, Rossi A. Spontaneously regressing leukoencephalopathy with bilateral temporal cysts in congenital rubella infection. The Pediatric Infectious Disease Journal. 2014;**33**(4):422-424

[37] Steinlin MI, Nadal D, Eich GF, Martin E, Boltshauser EJ. Intrauterine cytomegalovirus infection: Clinical and neuroimaging findings. Pediatric Neurology. 1996;**15**(3):249-253. DOI: 10.1016/s0887-8994(96)00170-1

[38] Groenendaal F, de Vries LS. Fifty years of brain imaging in neonatal encephalopathy following perinatal asphyxia. Pediatric Research. 2017;**81**(1-2):150-155

[39] Fitzgerald MP, Reynolds A, Garvey CM, Norman G, King MD, Hayes BC. Hearing impairment and hypoxia ischaemic encephalopathy: Incidence and associated factors. European Journal of Paediatric Neurology. 2019;**23**(1):81-86

[40] Shibasaki J, Aida N, Morisaki N, Tomiyasu M, Nishi Y, Toyoshima K. Changes in brain metabolite concentrations after neonatal hypoxic-ischemic encephalopathy. Radiology. 2018;**288**(3):840-848

[41] Lucke AM, Shetty AN, Hagan JL, et al. Early proton magnetic resonance spectroscopy during and after therapeutic hypothermia in perinatal hypoxic-ischemic encephalopathy. Pediatric Radiology. 2019;**49**:941-950. DOI: 10.1007/s00247-019-04383-8